© 2014. Published by The Company of Biologists Ltd | Development (2014) 141, 4448-4456 doi:10.1242/dev.113654

RESEARCH ARTICLE

STEM CELLS AND REGENERATION

Downregulation of miR122 by grainyhead-like 2 restricts the hepatocytic differentiation potential of adult liver progenitor cells

Naoki Tanimizu*, Seiji Kobayashi, Norihisa Ichinohe and Toshihiro Mitaka

ABSTRACT

Late fetal and adult livers are reported to contain bipotential liver stem/progenitor cells (LPCs), which share surface markers, including epithelial cell adhesion molecule (EpCAM), with cholangiocytes and differentiate into both hepatocytes and cholangiocytes. However, recent results do not necessarily support the idea that LPCs contribute significantly to cellular turnover and regeneration by supplying new hepatocytes. Here, we examined the colony-forming capability of EpCAM$^+$ cells isolated from mouse livers between E17 and 11 weeks of age. We found that the number of bipotential colonies was greatly reduced between 1 and 6 weeks, indicating that the number of LPCs decreases during postnatal development. Moreover, bipotential colonies derived from adult LPCs contained substantially fewer albumin$^+$ cells than those from neonatal LPCs. We further examined the differentiation potential of neonatal and adult LPCs by transplantation and found that neonatal cells differentiated into mature hepatocytes in recipient livers more frequently than adult LPCs. Since we previously reported that the transcription factor grainyhead-like 2 (GRHL2) expressed in EpCAM$^+$ cells inhibits hepatocytic differentiation, we examined whether targets of GRHL2 might block hepatocytic differentiation. DNA and microRNA microarrays revealed that miR122, the expression of which correlates with hepatocytic differentiation, was greatly reduced in adult as compared with neonatal EpCAM$^+$ cells. Indeed, GRHL2 negatively regulates the promoter/enhancer activity of the *Mir122* gene. Our results indicate that neonatal but not adult EpCAM$^+$ LPCs have great potential to produce albumin$^+$ hepatocytes. GRHL2 suppresses transcription of miR122 and thereby restricts the differentiation potential of adult LPCs.

KEY WORDS: Tissue stem/progenitor cells, Bipotential, Postnatal development, Hepatocyte, Cholangiocyte, Transcription factor

INTRODUCTION

Many developing organs contain multipotent tissue-specific stem/progenitor cells that may be extinguished later in development (Zhou et al., 2007; Pan et al., 2013). Conversely, tissue-specific stem/progenitor cells are thought to contribute to supplying cellular components in mature organs for the maintenance of organ homeostasis and for recovery from injury. In some adult tissues/organs, such as the intestine and skin, it has been shown that residential stem/progenitor cells continuously produce multiple cell types in homeostasis (Fuchs, 2009; Barker et al., 2010). In many epithelial tissues and organs, however, it is not clear whether tissue-specific stem/progenitor cells actually contribute to cellular turnover throughout life.

The liver contains two types of epithelial cells, namely hepatocytes and cholangiocytes (biliary epithelial cells), which originate from fetal liver stem/progenitor cells (LPCs) termed hepatoblasts (Oertel et al., 2003; Tanimizu et al., 2003). Under severe chronic liver injury the ability of hepatocytes and/or cholangiocytes to multiply is exhausted, and then adult LPCs may be activated to supply these cell types. In addition to LPCs in regenerating livers, it has been reported that adult LPCs exist in the normal liver. Adult LPCs have been enriched in cellular fractions and express cholangiocyte markers, including epithelial cell adhesion molecule (EpCAM), CD133 (also known as PROM1), CD13 (also known as ANPEP), SRY-related HMG box transcription factor 9 (SOX9) and osteopontin (OPN; also known as SPP1) (Suzuki et al., 2008; Kamiya et al., 2009; Okabe et al., 2009; Cardinale et al., 2011; Dorrell et al., 2011; Furuyama et al., 2011; Español-Suñer et al., 2012). By genetic lineage tracing it was demonstrated that SOX9$^+$ LPCs forming the ductal plate, which constitutes the primitive structure of the bile duct, actually supplied cholangiocytes as well as mature hepatocytes (MHs) (Carpentier et al., 2011). By contrast, recent results showed that adult LPCs barely supplied MHs in normal liver (Malato et al., 2011; Español-Suñer et al., 2012). These results suggest that LPCs may exist in or near bile ducts and that LPCs might alter their differentiation potential during development.

In this study, we used EpCAM as a marker to enrich LPCs, which form bipotential colonies in a clonal condition. We found that neonatal EpCAM$^+$ LPCs produce hepatocytes much more efficiently than adult LPCs. We further demonstrated that grainyhead-like 2 (GRHL2), a cholangiocyte-specific transcription factor, downregulates miR122, a microRNA (miRNA) known to be important for hepatocytic differentiation. Thus, our data indicate that one crucial transcription factor is involved in defining the differentiation capability of epithelial tissue-specific stem/progenitor cells.

RESULTS

Isolation of LPCs from late-fetal and neonatal livers

It has been reported that the number of hepatoblasts (fetal LPCs) decreases from mid- to late fetal stage (Suzuki et al., 2002), that adult LPCs exist in livers beyond 2 weeks after birth, and that their number decreases during postnatal development (Kamiya et al., 2009). In accordance with a previous report (Okabe et al., 2009), we used EpCAM as a marker to enrich adult-type LPCs. We immunohistochemically confirmed that EpCAM$^+$ cells are localized next to the portal vein after E17 (Fig. 1A). A single-cell suspension was used to isolate single EpCAM$^+$ cells from the CD45$^-$ TER119$^-$ CD31$^-$ non-hematopoietic/non-endothelial cell fraction (Fig. 1B). As shown in Fig. 1C, EpCAM$^+$ cells formed bipotential colonies containing albumin (ALB)$^+$ hepatocytes and CK19$^+$ cholangiocytes. Interestingly, 1-week EpCAM$^+$ cells formed bipotential colonies most efficiently (Table 1 and Fig. 1D). By contrast, EpCAM$^+$ cells

Department of Tissue Development and Regeneration, Research Institute for Frontier Medicine, Sapporo Medical University School of Medicine, S-1, W-17, Chuo-ku, Sapporo 060-8556, Japan.

*Author for correspondence (tanimizu@sapmed.ac.jp)

Received 31 May 2014; Accepted 10 September 2014

Development (2014) 141, 4448-4456 doi:10.1242/dev.113654

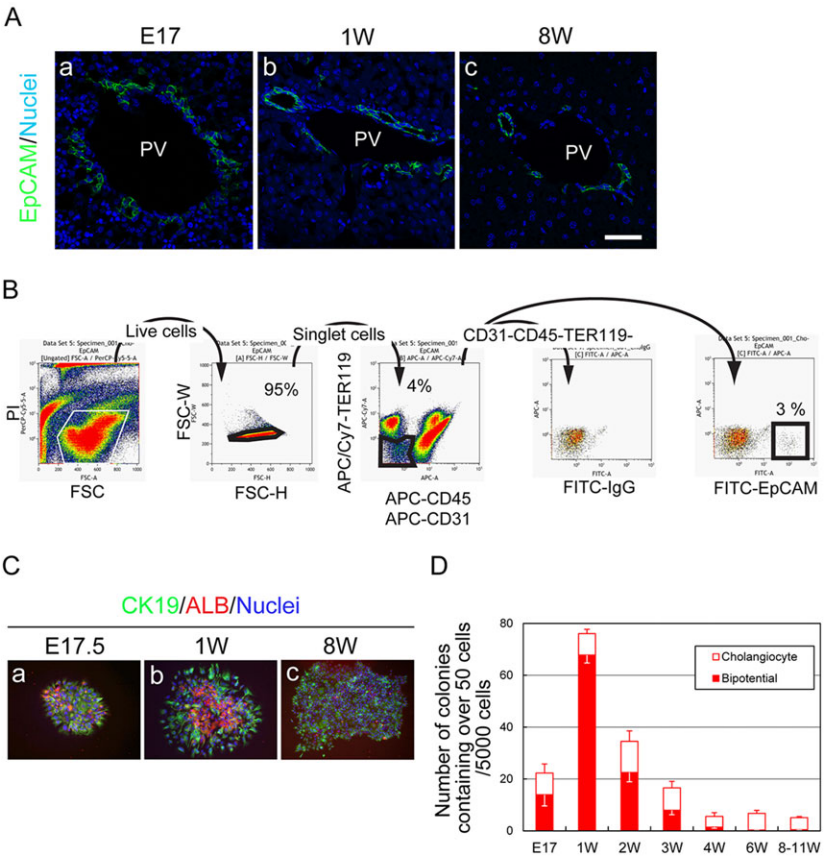

Fig. 1. Colony formation by EpCAM$^+$ cells at different developmental stages. (A) Expression of EpCAM in E17, 1-week (1W) and 8-week (8W) livers. EpCAM expression (green) is observed in primitive duct structures in E17 liver, whereas it is expressed in bile ducts in 1W and 8W livers. Scale bar: 50 µm. PV, portal vein. (B) Isolation of EpCAM$^+$ cells. Single EpCAM$^+$ cells were isolated from the CD45$^-$ TER119$^-$ CD31$^-$ fraction, which contains non-hematopoietic/non-endothelial cells, by FACS. Density plots for EpCAM$^+$ cell isolation from neonatal livers are shown. (C) Bipotential colonies derived from E17, 1W and 8W EpCAM$^+$ cells. Purified EpCAM$^+$ cells were plated at a low cell density. Typical bipotential colonies containing both ALB$^+$ CK19$^-$ hepatocytes (red) and ALB$^-$ CK19$^+$ cholangiocytes (green) are shown. Bipotential colonies also contain ALB$^+$ CK19$^+$ cells. Nuclei were counterstained with Hoechst 33258. (D) Number of colonies derived from EpCAM$^+$ cells at different development stages. Bipotential colonies were apparently formed from EpCAM$^+$ cells by 4 weeks after birth. Thereafter, bipotential colonies were formed only to a limited degree from EpCAM$^+$ cells. Colonies containing ALB$^+$ CK19$^-$, ALB$^+$ CK19$^+$, and ALB$^-$ CK19$^+$ cells were counted as bipotential colonies, whereas those only containing ALB$^-$ CK19$^+$ cells were counted as cholangiocyte colonies. Top error bars indicate s.e.m. for the number of bipotential colonies, whereas bottom error bars indicate s.e.m. for cholangiocyte colonies.

isolated from 6- to 11-week livers mostly formed cholangiocyte colonies containing only CK19$^+$ cells (Fig. 1D). These results are consistent with a previous report demonstrating that the number of LPCs possessing the ability to form bipotential colonies decreases during postnatal development (Kamiya et al., 2009). In addition, we noted that the ratio of ALB$^+$ to total colony-forming cells was much lower in bipotential colonies derived from 8-week versus 1-week EpCAM$^+$ cells (Fig 1Cb,c). This suggests that, in addition to a reduction in LPC numbers, the hepatocytic differentiation potential of LPCs might decrease as postnatal development progresses.

To further compare the differentiation capability of neonatal and adult LPCs, we examined the ratio of ALB$^+$ cells, including both ALB$^+$ CK19$^-$ and ALB$^+$ CK19$^+$, among colony-forming cells (Fig. 2A). The results indicated that more than 50% of cells were ALB$^+$ in colonies derived from 1-week EpCAM$^+$ cells (neonate) as compared with only ~10% of cells in colonies derived from 6-week EpCAM$^+$ cells (adult).

Table 1. Colony formation from EpCAM$^+$ cells isolated from developing livers

	Small (<50 cells)		Large (≥50 cells)	
Age	Bipotential	Cholangiocytic	Bipotential	Cholangiocytic
E17	11.7±5.6	20.7±5.3	13.9±4.3	8.4±4.2
1W	24.6±1.7	9.8±1.4	67.8±3.1	8.3±1.4
2W	12.5±4.1	9.0±1.7	22.5±3.6	12.0±3.4
3W	3.5±1.8	2.8±0.6	8.0±1.7	8.6±2.5
4W	1.0±0.4	4.5±0.8	1.7±0.4	6.3±1.1
6W	0.3±0.1	6.1±1.3	0.3±0.1	6.4±1.2
8-11W	0.1±0.1	2.3±0.4	0.4±0.2	4.7±0.4

The numbers of colonies containing fewer than 50 cells (small) and more than 50 cells (large) per 5000 EpCAM$^+$ cells are shown as the average±s.e.m. For each experiment n=6-8 mice for E17-2W and n=3 mice for 3W-11W. The colony assay was repeated at least three times. E, embryonic day; W, week.

Next, we analyzed the level of albumin expression in each bipotential colony. For this purpose, we prepared cDNA from total RNA extracted from each colony and examined whether each colony expresses albumin (Fig. 2C). We then selected albumin$^+$ colonies and quantified the albumin expression level. The level of albumin expression was much higher in neonatal bipotential colonies than in adult colonies (Fig. 2D). Expression of *Ck19* (*Krt19*), *Sox9* and *Epcam* was relatively low in colonies expressing albumin at high level.

Neonatal LPCs differentiate to hepatocytes *in vitro* and *in vivo*

To further clarify whether neonatal and adult LPCs can differentiate into hepatocytes, we subcultured colonies derived from EpCAM$^+$ cells isolated from 1-week and 6-week livers. We picked up ten colonies of each and successfully established four and five clones from 1-week and 6-week colonies, respectively. Two out of four neonatal clones (clones 2 and 4) retained the original marker EpCAM, whereas it was eventually lost from the other clones (data not shown).

We induced hepatocytic differentiation of LPC clones by oncostatin M (OSM) and Matrigel (MG). After induction, all neonatal clones expressed marker genes related to differentiated functions of hepatocytes, including metabolic enzymes and cytochrome P-450s (Fig. 3A). By contrast, adult clones were induced to express only albumin and carbamoyl-phosphate synthetase 1 (*Cps1*). We quantified the expression level of *Cps1* and tyrosine aminotransferase (*Tat*) and the data showed that neonatal clones expressed both genes at a level comparable to

Development (2014) 141, 4448-4456 doi:10.1242/dev.113654

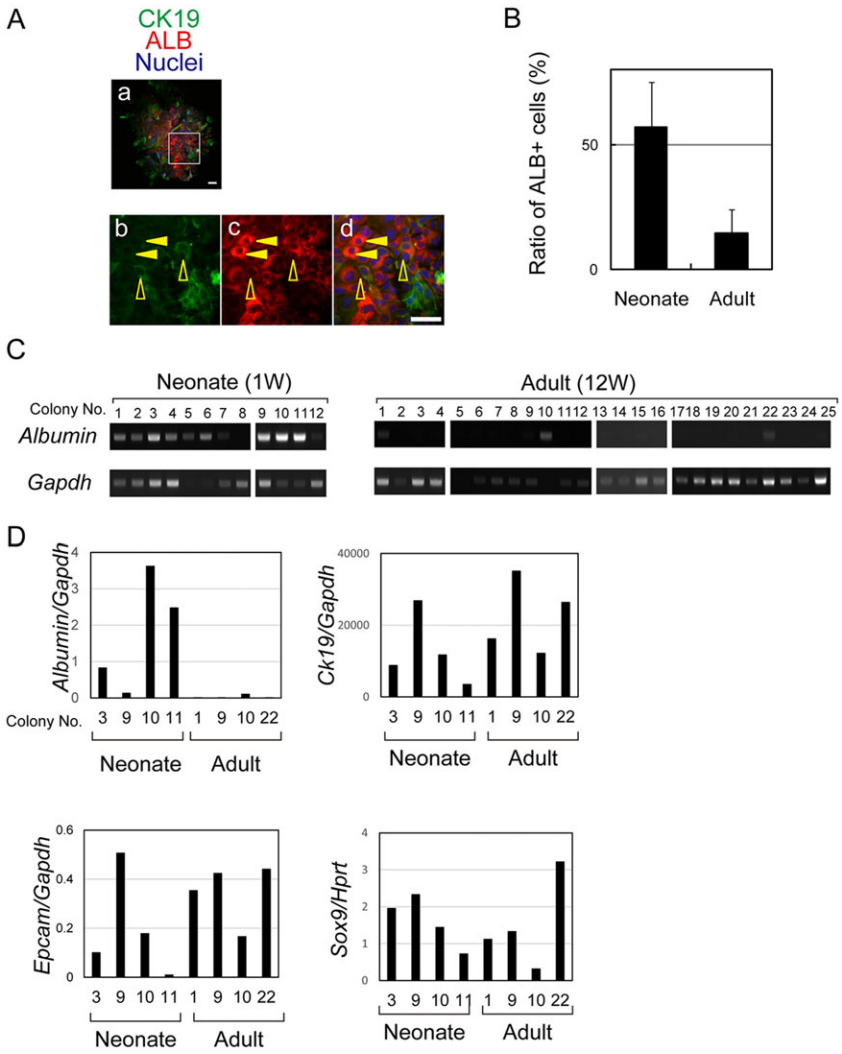

Fig. 2. Neonatal and adult LPCs differ in their potential to produce albumin$^+$ hepatocytes. (A) Bipotential colonies contain two types of hepatocytic cells: ALB$^+$ CK19$^-$ (solid arrowheads) and ALB$^+$ CK19$^+$ (open arrowheads) cells. A bipotential colony derived from a neonatal EpCAM$^+$ cell is shown (a), with the boxed area magnified to show individual and merged channels (b-d). Scale bars: 50 μm. (B) Ratio of ALB$^+$ cells among total cells in each colony. More than 50% and ~10% of cells are ALB$^+$ in each neonatal and adult colony, respectively. Error bars indicate s.e.m. (C) Albumin expression in each colony. Low cell density culture was performed for 2 weeks. Total RNA extracted from each colony was used to synthesize cDNA to examine albumin expression by PCR. Colonies positive for albumin were considered to be derived from LPCs. *Gapdh* provides a control. (D) Quantitative analysis of albumin, *Ck19*, *Epcam* and *Sox9* expression in each colony. Four albumin$^+$ neonatal colonies were selected, while all four albumin$^+$ adult colonies were used to quantify the expression level of albumin and *Ck19*. Neonatal bipotential colonies express more albumin than adult colonies. The expression levels of *Ck19* are similar in neonatal and adult colonies. Relative expression levels compared with that of mature hepatocytes (MHs), which were cultured for 1 day, are shown.

MHs (Fig. 3B). Neonatal cells showed hepatocytic morphology after induction (Fig. 3Ca,b). Furthermore, the expression of hepatocyte nuclear factor 4α (HNF4α), CCAAT/enhancer binding protein α (C/EBPα), ALB and CPS1 was induced in neonatal clones (Fig. 3Ca-h). Neither morphological changes nor the expression of HNF4α and ALB was clearly induced in adult clones (Fig. 3Ci-m). These results further support the proposal that neonatal LPCs have greater potential than adult LPCs to differentiate into hepatocytes.

In order to examine the differentiation capability of neonatal and adult LPCs *in vivo*, we transplanted neonatal and adult clones. All the clones were labeled with GFP, and GFP$^+$ cells were enriched by FACS (Fig. 4A). Recipient mice were pretreated with retrorsine, which inhibits hepatocyte proliferation, and then 70% partial hepatectomy was performed at the time of transplantation (Fig. 4B). Recipient liver sections were stained with anti-GFP antibody to identify donor cells (Fig. 4C). Engraftments of donor cells were observed in recipients transplanted with either neonatal or adult clones (Table 2). Neonatal clones were engrafted as hepatocytic or ductular cells (Fig. 4Ca,b). By contrast, the engraftment of adult cells was rare and these were mostly found as ductular cells (Fig. 4Cc).

We further examined the recipient livers transplanted with neonatal cells by expression of hepatocyte and cholangiocyte markers (Fig. 4D). Neonatal clones differentiated to HNF4α$^+$ hepatocytes or CK19$^+$ cholangiocytes (Fig. 4Da-d). Since recipient CD31$^+$ sinusoidal endothelial cells entered into a cluster of HNF4α$^+$ donor cells, donor-derived hepatocytes were incorporated into recipient liver trabeculae (Fig. 4De-h). We also examined the expression of hepatocyte and cholangiocyte markers in recipient livers transplanted with adult cells and found that most of the donor cells differentiated to CK19$^+$ ductular cells (Fig. 4Ea-d). The GFP$^+$ ductular structure (dotted circle in supplementary material Fig. S1a-c) was separate from the portal veins (asterisks in supplementary material Fig. S1). The differentiated cells also expressed other cholangiocyte markers (supplementary material Fig. S1f-w). A small proportion of donor cells became CK19$^+$ HNF4α$^+$ cells, which did not form the ductular structure (Fig. 4Ee). These results indicate that EpCAM$^+$ LPCs show bidirectional differentiation capability *in vivo*, although adult LPCs rarely differentiate into hepatocytes.

These results further support the proposal that the bipotency of LPCs is altered during development. Thus, we considered that a molecular machinery restricting the differentiation potential might exist in adult LPCs.

Comparison between neonatal and adult EpCAM$^+$ cells

It has been demonstrated that certain transcription factors are crucial in defining cellular lineages. We previously found that cholangiocyte transcription factors, including GRHL2 and SOX9, are expressed at a higher level in adult than in neonatal EpCAM$^+$ cells (Tanimizu et al., 2013). However, we had not examined

Development (2014) 141, 4448-4456 doi:10.1242/dev.113654

whether neonatal EpCAM$^+$ cells equally expressed these markers at low level or if they contain cells positive and negative for the markers. We prepared smear samples of FACS-purified EpCAM$^+$ cells and examined the expression of HNF1β, SOX9, GRHL2 and HNF4α, as well as CK19 and OPN in each neonatal and adult EpCAM$^+$ cell (Table 3). Consistent with the data in Table 3, HNF1β, SOX9 and OPN, but not HNF4α, are expressed in neonatal and adult EpCAM$^+$ cells in liver tissues (supplementary material Figs S2 and S3). Interestingly, ~25% of neonatal EpCAM$^+$ cells were GRHL2$^-$ (Fig. 5Aa-c), whereas the adult EpCAM$^+$ fraction barely contained any GRHL2$^-$ cells (Fig. 5Ad-f).

We further confirmed that neonatal EpCAM$^+$ cells were GRHL2$^+$ (Fig. 5Bb-d) or GRHL2$^-$ (Fig. 5Be-g) by examining its expression in neonatal liver sections. Neonatal EpCAM$^+$ GRHL2$^-$ cells formed smaller ductules in the periphery. By contrast, bile ducts in the adult liver consist of EpCAM$^+$ GRHL2$^+$ cells (Fig. 5Bh-n). Additionally, the expression pattern of CK19 was similar to that of GRHL2 (supplementary material Fig. S3). Previously, we demonstrated that GRHL2 not only promotes the maturation of cholangiocytes but also inhibits hepatocytic differentiation (Tanimizu et al., 2013). Therefore, these results suggest that substantial differences in differentiation potential might exist among neonatal EpCAM$^+$ cells, as well as between neonatal and adult cells. We further examined the possibility that GRHL2 expression might regulate the hepatocytic differentiation potential of LPCs.

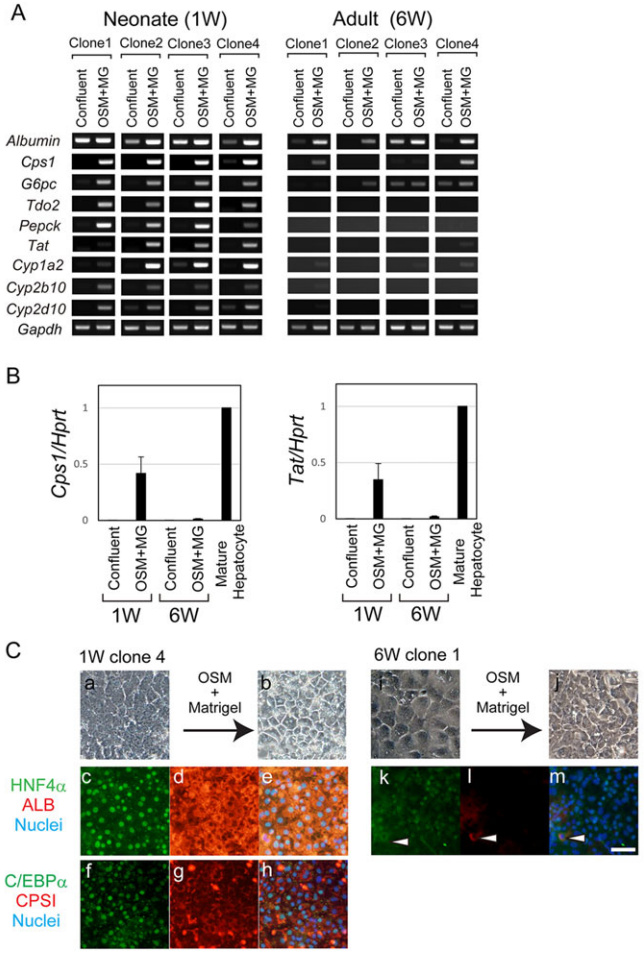

Fig. 3. Neonatal EpCAM$^+$ LPCs efficiently differentiate to functional hepatocytes *in vitro*. (A) Expression of hepatocyte markers in cultures of neonatal and adult clones. Neonatal and adult LPC clones were induced to differentiate into hepatocytes by sequential treatment with oncostatin M (OSM) and Matrigel (MG). Expression of marker genes was examined by PCR. In neonatal cultures, metabolic enzymes and cytochrome P-450s were induced. (B) Expression level of *Cps1* and *Tat* in neonatal and adult LPCs after hepatocytic differentiation. Both *Cps1* and *Tat* were induced much more in neonatal than in adult cells. The average values from four clones are shown. Error bars represent s.e.m. (C) Hepatocytic differentiation of neonatal and adult clones. Morphology of neonatal clone 4 shows round nuclei and dense cytoplasm after inducing hepatocytic differentiation (a,b). Expression of the hepatocyte markers HNF4α, C/EBPα, ALB and CPS1 is detectable (c-h). By contrast, cells of adult clone 1 do not show hepatocytic morphology even after inducing hepatocytic differentiation (i,j). Expression of HNF4α is weakly observed. A cell positive for ALB is seen (arrowhead) but it is negative for nuclear HNF4α (k-m). Scale bar: 50 μm.

GRHL2 suppresses the expression of miR122

To correlate the expression profile of GRHL2 with the bipotency of LPCs, we examined its expression in colonies derived from neonatal and adult EpCAM$^+$ cells. We found that intense and uniform expression of GRHL2 was maintained in colonies derived from adult EpCAM$^+$ cells (Fig. 6Aa-e). By contrast, neonatal EpCAM$^+$ cells formed two types of colonies: one consisted of GRHL2$^-$ cells (Fig. 6Af-j) and the other of GRHL2$^+$ and GRHL2$^-$ cells (Fig. 6Ak-o). Although the neonatal GRHL2$^-$ and GRHL2$^+$ colonies were similar in size, the GRHL2$^-$ colonies contained more ALB$^+$ cells (Fig. 6B). In addition, in GRHL2$^+$ colonies ALB was restricted to cells in which GRHL2 was spontaneously downregulated (Fig. 6C). Based on these results, we considered the possibility that targets of GRHL2 might be involved in reducing the hepatocytic differentiation potential of LPCs.

To identify molecules downstream of GRHL2, we performed mRNA and miRNA microarray analyses using a hepatic progenitor cell line HPPL with or without GRHL2. Since HPPL cells do not express GRHL2, we expected that its targets would be clearly upregulated or downregulated in HPPL cells with GRHL2. The results of the mRNA microarray suggested that some metabolic genes, such as arginase and *Cps1* were downregulated by overexpression of GRHL2. The results of the miRNA microarray, by contrast, suggested that miR122 was remarkably downregulated by GRHL2 (Table 4; supplementary material Table S3). We confirmed this result by quantitative PCR analysis, showing that overexpression of GRHL2 substantially downregulated miR122 in HPPL cells (Fig. 7A).

It has been reported that miR122 is important for hepatocytic differentiation (Laudadio et al., 2012). Consistently, overexpression of GRHL2 in HPPL cells, in which miR122 was downregulated (Fig. 7A), inhibited hepatocytic differentiation (supplementary material Fig. S4). We also found that knockdown of GRHL2 increased miR122 in adult EpCAM$^+$ cells (Fig. 7B). We further examined the effect of miR122 on hepatocytic differentiation by introducing a miR122 mimic, and found that it slightly upregulated albumin and downregulated *Ck19* in colonies derived from adult EpCAM$^+$ cells (Fig. 7C). We also found that the miR122 mimic upregulated albumin, *Cps1* and *Tat* but not *Hnf4a* in primary EpCAM$^+$ cells (supplementary material Fig. S5). Consistent with the notion that the Notch signaling pathway promotes cholangiocyte differentiation (Tanimizu and Miyajima, 2004; Zong et al., 2009), DAPT, which is a γ-secretase inhibitor and thereby a potent inhibitor of the Notch signaling pathway, further promoted upregulation of *Cps1* and *Tat* by miR122 (supplementary material Fig. S5). Consistent with their reduced capacity to differentiate into hepatocytes, miR122 expression in adult EpCAM$^+$ cells was significantly lower than in neonatal cells, whereas *Grhl2* expression in adult cells was higher than in neonatal cells (Fig. 7D). Furthermore, in neonatal and adult LPC colonies, *Grhl2* and *Mir122* expression levels are negatively

Development (2014) 141, 4448-4456 doi:10.1242/dev.113654

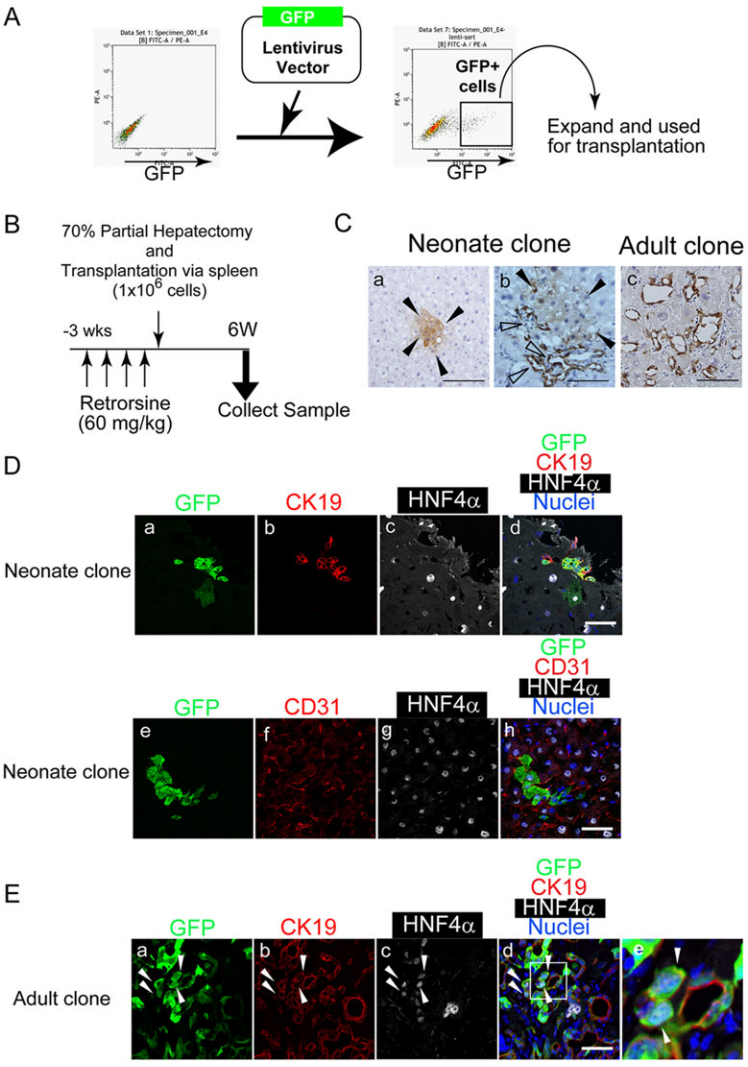

Fig. 4. Engraftment of neonatal and adult LPCs in recipient livers. (A) Preparation of GFP$^+$ LPCs. LPC clones were infected with lentivirus containing the *GFP* gene. GFP$^+$ cells were isolated by FACS and expanded before transplantation. (B) Timecourse of retrorsine treatments, partial hepatectomy and transplantation. (C) GFP$^+$ cells are detected in recipient livers. Neonatal clones are detected as hepatocytic cells (solid arrowheads in a,b) as well as ductular cells (open arrowheads in b). Adult donor cells are mostly observed as ductular cells (c). Images represent recipient livers transplanted with neonatal clone 2 (a), neonatal clone 4 (b) and adult clone 1 (c). GFP expression was detected by DAB staining. (D) Neonatal LPC clones differentiate into HNF4α$^+$ hepatocytes and CK19$^+$ cholangiocytes in the recipient liver. Recipient liver sections were stained with anti-GFP, anti-CK19 and anti-HNF4α (a-d) or with anti-GFP, anti-CD31 and anti-HNF4α (e-h) antibodies. GFP$^+$ donor cells differentiate into CK19$^+$ cholangiocytes and HNF4α$^+$ hepatocytes in the recipient liver (a-d). GFP$^+$ HNF4α$^+$ hepatocytes are associated with recipient CD31$^+$ endothelial cells, indicating that donor-derived hepatocytes are incorporated into recipient liver tissue. Sections of a recipient liver transplanted with neonatal clone 4 are shown. Nuclei were counterstained with Hoechst 33258. (E) Adult LPC clone differentiates to CK19$^+$ cholangiocytes in the recipient liver. A frozen section of recipient liver transplanted with adult clone 1 was stained with anti-GFP, anti-CK19 and anti-HNF4α. GFP$^+$ donor cells express CK19 and form ductular structures. Some GFP$^+$ CK19$^+$ cells are positive for HNF4α$^+$ (arrowheads) and are not incorporated into ductular structure (e, which is a magnification of the boxed region in d). Nuclei were counterstained with Hoechst 33258. Scale bars: 100 μm in C; 50 μm in D,E.

and positively correlated with albumin expression, respectively (supplementary material Fig. S6). These results further support the hypothesis that downregulation of miR122 by GRHL2 is one of the key molecular pathways restricting the hepatocytic differentiation potential of LPCs.

It has been reported that *Mir122* expression is controlled by the proximal promoter and enhancers (Xu et al., 2010; Laudadio et al., 2012). In order to determine whether GRHL2 transcriptionally regulates *Mir122*, we examined its effect on reporter constructs containing the *Mir122* proximal promoter/enhancer (Fig. 7E). The results indicate that GRHL2 negatively regulates *Mir122* promoter/enhancer activity.

Table 2. Efficiency of cell transplantation

Clone	Donor cell occurrence‡	Donor cell spots/cm^2	
		With hepatocytic features	With ductular features
Neonate clone 2	4/4	0.94±0.24*	0.19±0.09*
Neonate clone 4	3/3	1.4±0.3**	1.4±0.1**
Adult clone 1	1/3	0.11±0.04	0.77±0.39
Adult clone 4	0/2	–	–

For each recipient liver, 8-12 sections were prepared and examined for GFP$^+$ cells. Clusters containing more than two GFP$^+$ cells were counted as donor cell spots. Statistical analysis showed that neonatal clones were engrafted as hepatocytes more efficiently than adult clones (neonatal clone 2 versus adult clone 1, *P=0.026; neonatal clone 4 versus adult clone 1, **P=0.045).
‡Number of mice with GFP$^+$ donor cells/total number of mice transplanted.

DISCUSSION

Each tissue/organ may contain tissue-specific stem/progenitor cells that contribute to organogenesis, homeostasis and the recovery from injury. However, it remains unclear whether tissue stem/progenitor cells retain the same differentiation potential throughout life. In this study, by examining characteristics of LPCs continuously between late fetal and adult periods, we demonstrate that the number of LPCs and their differentiation capability are restricted during postnatal liver development. We further identified that downregulation of miR122 by GRHL2 is one of the molecular pathways regulating the differentiation capability of LPCs.

We have shown (Fig. 7) that miR122 alone can increase the expression of albumin in adult LPCs. However, given that overexpression of GRHL2 remarkably inhibited hepatocytic differentiation (supplementary material Fig. S4), the effect of miR122 on hepatocytic differentiation is relatively weak. We previously found that overexpression of GRHL2 inhibited the expression of HNF4α in neonatal EpCAM$^+$ cells, which key to suppressing hepatocytic differentiation. However, introduction of a miR122 mimic did not significantly increase *Hnf4a* expression in

Development (2014) 141, 4448-4456 doi:10.1242/dev.113654

Table 3. Expression of cholangiocyte and hepatocyte markers in neonatal and adult EpCAM$^+$ cells

	CK19		GRHL2		HNF1β		OPN		SOX9		ALB		HNF4α	
	–	+	–	+	–	+	–	+	–	+	–	+	–	+
Neonate														
%	4.4	95.6	26	74	1.3	98.7	1.0	99	3.0	97.0	97.7	2.3	0.8	99.2
n	250		373		78		102		562		526		634	
Adult														
%	0	100	1.8	98.2	0.9	99.1	0	100	1.8	98.2	99.3	0.7	100	0
n	155		227		218		234		227		424		112	

EpCAM$^+$ cells were isolated from neonatal and adult livers by FACS, smear samples were prepared and used for immunostaining. The indicated number of EpCAM$^+$ cells were examined for expression of each marker. Ratios of marker-negative and marker-positive cells are shown.

adult EpCAM$^+$ cells (supplementary material Fig. S5). Taken together, we consider that, in addition to miR122, other downstream targets of GRHL2 also participate in modulating the differentiation potential of LPCs.

LPCs have been thoroughly characterized beyond 2 weeks after birth (Kamiya et al., 2009). In addition, by examining the differentiation potential of late fetal, neonatal and adult LPCs, we found that neonatal LPCs showed a strong ability to differentiate into functional hepatocytes *in vitro* and *in vivo*, suggesting that EpCAM$^+$ LPCs are a candidate for supplying hepatocytes during early postnatal development as embryonic ductal plate cells (Carpentier et al., 2011). However, since hepatocytes show the ability to proliferate even in a clonal condition by 4 weeks (data not shown), they certainly play an important role in supplying new hepatocytes during early postnatal development. Therefore, further experiments are necessary to prove whether neonatal EpCAM$^+$ LPCs also supply new hepatocytes during development.

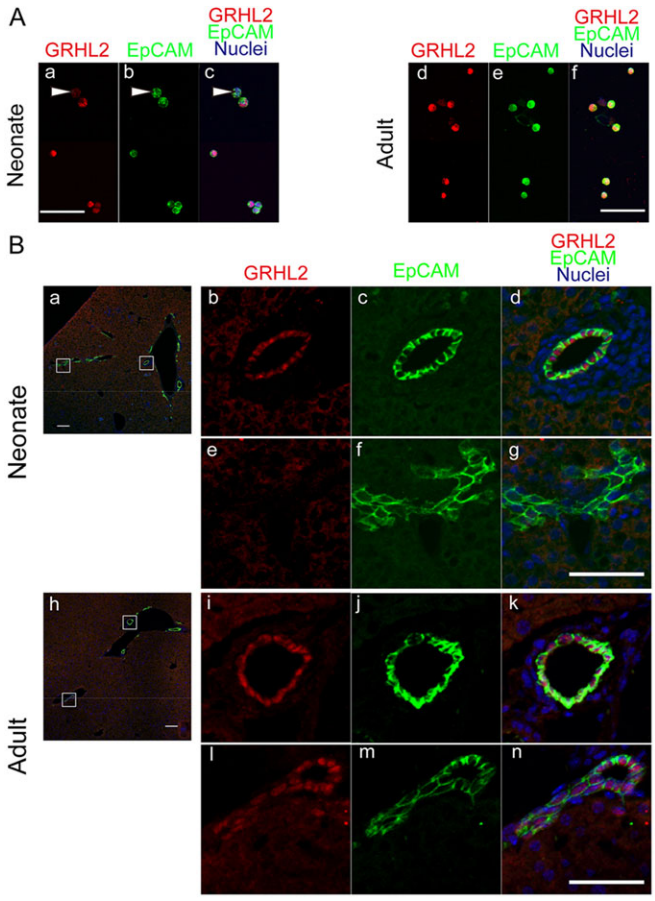

Fig. 5. Expression of GRHL2 in adult and neonatal EpCAM$^+$ cells. (A) The neonatal EpCAM$^+$ fraction contains GRHL2$^+$ and GRHL2$^-$ cells. Some neonatal EpCAM$^+$ cells are GRHL2$^-$ (arrowhead in a-c), whereas adult EpCAM$^+$ cells do not contain GRHL2$^-$ cells (d-f). EpCAM$^+$ cells were isolated by FACS and used to prepare smear samples. (B) EpCAM$^+$ GRHL2$^-$ and EpCAM$^+$ GRHL2$^+$ cells form bile ducts in neonatal livers. In neonatal liver, bile ducts associated with a clear lumen express GRHL2 (b-d), whereas it is not expressed by some of the small ductules (e-g). By contrast, GRHL2 is expressed in small ductules (l-n) as well as large ducts (i-k) in adult liver. Boxed regions in a and h are enlarged in b-g and i-n, respectively. Scale bars: 50 μm in A and Bg,n; 100 μm in Ba,h.

Adult LPCs have been enriched in cellular fractions that are positive for cholangiocyte markers and they have potential to differentiate to hepatocytes *in vitro* and *in vivo* (Suzuki et al., 2008; Okabe et al., 2009; Cardinale et al., 2011; Dorrell et al., 2011; Furuyama et al., 2011; Español-Suñer et al., 2012). Consistent with previous work, we demonstrated that adult LPCs are enriched in the EpCAM$^+$ fraction. However, compared with 1-week LPCs, their capability to differentiate into hepatocytes was very low. Given that recent lineage-tracing studies failed to detect MHs derived from LPCs *in vivo* without injury (Español-Suñer et al., 2012), the differentiation capability of LPCs appears extremely limited at the late postnatal and adult period. Specific stimulation, including Wnt plus R-spondin (Huch et al., 2013), and/or inhibition of the Notch signal (Boulter et al., 2012) might be necessary to release adult LPCs from the molecular machineries that serve to block hepatocytic differentiation.

By examining the expression of marker genes at the single-cell level, we found that neonatal EpCAM$^+$ cells can be divided into GRHL2$^-$ and GRHL2$^+$. Interestingly, EpCAM$^+$ GRHL2$^-$ cells formed small ductules in the periphery of the neonatal liver. According to the recent model of bile duct development, in which development/morphogenesis proceed from the liver hilum to the periphery (Antoniou et al., 2009), these EpCAM$^+$ GRHL2$^-$ cells might be recently committed from hepatoblasts and thereby retain bidirectional differentiation capability. In addition, in contrast to adult cells, neonatal EpCAM$^+$ GRHL2$^+$ cells spontaneously lose expression of GRHL2 and then express ALB during clonal expansion (Fig. 6C). Therefore, it can be assumed that GRHL2 expression is not necessarily fixed even in EpCAM$^+$ GRHL2$^+$ cells at neonatal stage, and, thereby, that neonatal EpCAM$^+$ GRHL2$^+$ cells retain the potential to differentiate into hepatocytes.

In this study, we demonstrated that neonatal and adult LPCs are distinct in terms of their hepatocytic differentiation potential. It has been demonstrated that the combination of GATA4, FOXA3 and HNF1α (Huang et al., 2011) or of HNF4α and one of the FOXA factors (Sekiya and Suzuki, 2011) converts fibroblasts into hepatocytes. By contrast, overexpression of HNF4α in the presence of endogenous FOXA1 did not induce hepatocytic characteristics in EpCAM$^+$ cells (Tanimizu et al., 2013). Given that recent reports

Development (2014) 141, 4448-4456 doi:10.1242/dev.113654

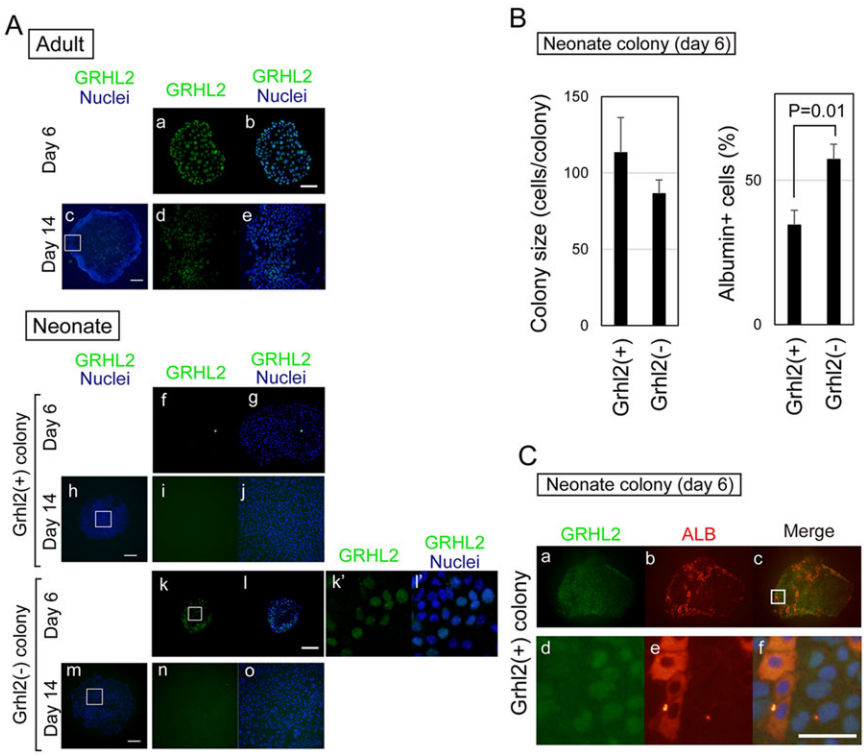

Fig. 6. Change in GRHL2 expression during clonal expansion of EpCAM$^+$ cells. (A) Adult LPCs maintain GRHL2 during clonal culture. GRHL2 is expressed in adult colonies at day 6 and 14 (a-e). By contrast, neonatal colonies are either GRHL2$^+$ (f-j) or GRHL2$^-$ (k-o). Boxed regions in c, h, m and k are enlarged in d,e, i,j, n,o and k′,l′, respectively. Scale bars: 500 µm in c,h,m; 100 µm in b,l. (B) GRHL2 expression does not affect the clonal proliferation of LPCs but their differentiation potential. Neonatal colonies were stained with anti-albumin, anti-GRHL2 antibody and Hoechst 33258. Total and albumin$^+$ cells in each colony were counted. Error bars represent s.e.m. (C) Expression of GRHL2 and ALB are mutually exclusive in neonatal GRHL2$^+$ colonies. The boxed region in c is magnified in d-f. Scale bar: 50 µm.

suggested that, even in chronically injured livers, LPCs do not efficiently supply new hepatocytes (Tarlow et al., 2014), adult LPCs might be equipped with molecular machineries blocking hepatocytic differentiation. The present finding that miR122 is downregulated by GRHL2 might provide an explanation for such mechanisms. Recently, it was demonstrated that key transcription factors defining neural lineage cells, including PAX6 and ETV6, inhibit dedifferentiation induced by OCT3/4 (POU5F1), SOX2, KLF4 and cMYC during reprograming (Hikichi et al., 2013). As we have previously demonstrated (Senga et al., 2012; Tanimizu et al., 2013), GRHL2 is a key transcription factor in inducing the cellular properties of mature cholangiocytes. Therefore, transcription factors conferring specific functions and/or structures to certain cell types might generally define the differentiation potential of tissue-specific stem/progenitor cells. In order to use highly proliferative LPCs *in vitro* and *in vivo* for the purposes of producing functional hepatocytes, it might be important to release them from inhibitory machineries in order to make them responsive to inductive signals for hepatocytic differentiation.

MATERIALS AND METHODS

Extracellular matrix, growth factors and chemicals

Growth factor-reduced Matrigel (MG) and purified laminin 111 were from BD Biosciences. Epidermal growth factor (EGF), hepatocyte growth factor (HGF) and oncostatin M (OSM) were purchased from R&D Systems.

Table 4. miRNAs downregulated by GRHL2 overexpression

miRNA	GRHL2 versus control
miR122	0.078
miR760-5P	0.29
miR192	0.35
miR194	0.38
miR181B	0.38

A liver progenitor cell line, HPPL, was introduced with *Grhl2* and the expression profile of miRNAs compared between HPPL (control) and HPPL-*Grhl2* by microarray.

C57BL6 and nude mice were purchased from Sankyo Labo Service Corporation (Tokyo, Japan). All animal experiments were approved by the Sapporo Medical University Institutional Animal Care and Use Committee and were carried out under the institutional guidelines for ethical animal use.

Cell isolation and sorting

E17 mouse livers were cut into small pieces and then digested in PBS containing Mg^{2+}, Ca^{2+} and Librase-TM (Roche Applied Sciences). For neonatal and adult mouse livers, a two-step collagenase perfusion method was used to isolate cells as previously reported (Tanimizu et al., 2013). Liberated cells were used to isolate EpCAM$^+$ cells by FACS. Non-specific binding of antibodies was blocked by antibody against Fcγ receptor (anti-CD16/CD32 antibody). Cells were labeled with FITC-conjugated anti-EpCAM, APC-conjugated anti-CD45 (PTPRC), APC-conjugated anti-CD31 (PECAM1) and APC-Cy7-conjugated anti-TER119 (LY76) antibodies, and with propidium iodide (PI; Sigma-Aldrich). EpCAM$^+$ cells were isolated from PI$^-$ live cells by FACS using a FACSAria II (BD Biosciences). Antibodies used are listed in supplementary material Table S1.

Colony assay

Single EpCAM$^+$ cells were isolated by FACSAria II as described above. Five to eight thousand cells were plated in a 35-mm dish coated with laminin 111 (BD Biosciences). The cells were cultured in DMEM/Fischer F-12 medium supplemented with 10% FBS, 10 ng/ml EGF, 10 ng/ml HGF, 0.1 µM dexamethasone (Dex; Sigma-Aldrich) and 1× insulin-transferrin-selenium (ITS; Gibco). After 9 days of culture, cells were fixed in 4% paraformaldehyde (PFA) and stained with anti-cytokeratin 19 (CK19) and anti-albumin antibodies (supplementary material Table S1). Signals were visualized with Alexa Fluor-conjugated secondary antibodies (Molecular Probes). Nuclei were counterstained with Hoechst 33258 (Dojindo). Images were acquired on a Nikon X-81 fluorescence microscope. Colonies containing more than 50 cells were categorized into three groups: bipotential colonies, which consist of ALB$^+$ hepatocytes and CK19$^+$ cholangiocytes; hepatocyte colonies, which consist of only ALB$^+$ cells; and cholangiocyte colonies, which consist of only CK19$^+$ cells. We define a cell that forms bipotential colonies as an LPC in the current study.

Development (2014) 141, 4448-4456 doi:10.1242/dev.113654

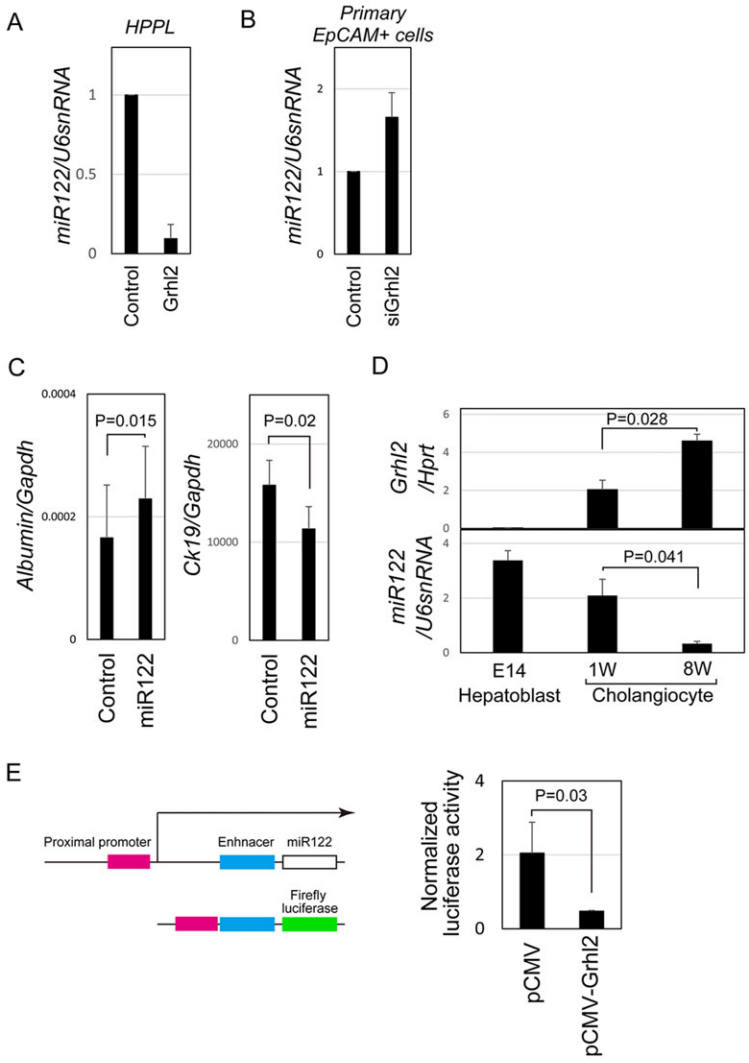

Fig. 7. GRHL2 downregulates miR122. (A) Quantitative analysis of miR122 expression in HPPL cells with or without GRHL2. (B) Quantitative analysis of miR122 expression in adult EpCAM$^+$ cells with or without RNAi against *Grhl2*. (C) miR122 upregulates and downregulates albumin and *Ck19*, respectively, in adult LPC colonies. Adult EpCAM$^+$ cells were cultured at low density for 2 weeks to allow them to form colonies. Each colony was picked and split into two wells of a 96-well plate for introduction of control or miR122 mimic. Two days later, expression of albumin and *Ck19* was examined by quantitative PCR. Relative expression levels against MHs cultured for 1 day were calculated. The average values from three colonies are shown. (D) Expression of miR122 during cholangiocyte differentiation. miR122 is significantly downregulated in EpCAM$^+$ cells during postnatal development. (E) Negative regulation of *Mir122* by GRHL2. *Mir122* promoter and enhancer sequences were linked to firefly luciferase and HEK293T cells were used to examine their activity in the absence and presence of GRHL2. GRHL2 was found to significantly downregulate the promoter/enhancer activity of *Mir122*. Error bars indicate s.e.m.

For establishing clones, each colony raised in the low density culture was treated with trypsin after being surrounded by a cloning ring (Asahi Glass Co., Tokyo, Japan). Cells were then plated in a well of a 24-well plate coated with laminin 111 and kept in the medium that was used for the colony assay. Expanded cells were replated every 4 days.

Induction of hepatocyte differentiation

To induce neonatal and adult LPC clones to differentiate to hepatocytes, 50,000 cells were plated on gelatin-coated wells of 24-well plates. After cells became confluent, they were incubated with 10 ng/ml OSM, 1% DMSO, 0.1 μM Dex and 1× ITS for 4 days and then overlaid with 5% MG for an additional 4 days. Stealth RNA against *Grhl2* (Invitrogen) and miR122 mimic (Ambion) were introduced into cells using RNAiMAX (Invitrogen).

PCR

Total RNA was isolated from purified EpCAM$^+$ cells using an RNeasy Mini Kit (Qiagen). cDNA was synthesized using the Omniscript Reverse Transcription Kit (Qiagen). Primers used for PCR are listed in supplementary material Table S2. TaqMan probes for *Hprt*, *Cps1*, *Grhl2*, miR122, *Sox9*, *Tat* and *U6 snRNA* were purchased from Applied Biosystems and used for quantitative PCR.

Cell transplantation

Nude mice were used for cell transplantation as described previously (Kamiya et al., 2009). LPC clone cells were labeled by GFP-encoding lentivirus vector and GFP$^+$ cells were isolated by FACSAria II. Recipient 4-week nude mice were intraperitoneally injected with 60 mg/kg retrorsine (Sigma-Aldrich) four times each week and then 70% of the liver was surgically removed at transplantation. GFP$^+$ cells (5×10^5-1×10^6) were injected into spleen. Six weeks after the transplantation, the liver was collected to examine the engraftment of donor cells. For detecting GFP$^+$ cells in recipient livers, frozen sections were incubated with anti-GFP antibody and then GFP signals were visualized using 3,3′-diaminobenzidine (DAB) (Sigma-Aldrich) as a chromogenic substrate for horseradish peroxidase, which was conjugated to anti-rabbit IgG antibody. Areas of sections were measured using Olympus CellSense Software.

Immunofluorescence

Liver tissues were fixed in PBS containing 4% PFA or in Zamboni solution at 4°C overnight. After washing in PBS and in PBS containing 20% sucrose, they were embedded in OCT compound (Sakura Finetek). Thin sections were prepared with a cryostat (CM1950, Leica Microsystems). After permeabilization with 0.2% Triton X-100 and blocking with Blockace (DS Pharma), sections were incubated with primary antibodies (supplementary material Table S1). Images were obtained with Zeiss 510 and 780 confocal microscopes.

Vector construction and luciferase assay

Grhl2 cDNA was amplified and inserted into a pcDNA3-myc vector, which was generated by inserting a myc-tag into pcDNA3 (Life Technologies). *Mir122* proximal promoter and enhancer sequences were amplified using mouse genomic DNA as a template and inserted into pUC118 vector (Takara Bio). The promoter and enhancer were inserted into the *Kpn*I/*Xho*I

Development (2014) 141, 4448-4456 doi:10.1242/dev.113654

sites of a pGL4.10 vector (Promega), which contained minimal TK promoter. HEK293T cells were co-transfected using pcDNA3 with or without *Grhl2*, pGL4.10 with or without *Mir122* promoter/enhancer, and a pRL-TK vector containing *Renilla* luciferase. At 48 h after transfection, luciferase activity was measured with the Dual-Luciferase Reporter Assay System (Promega) on an Infiniti M1000-Pro microplate reader (Tecan).

Statistical analysis

Statistical analyses to determine s.e.m. for colony assay, qPCR and luciferase assay and two-tailed Student's *t*-tests were performed using Excel (Microsoft).

Microarray analysis

Total RNA including microRNAs was extracted from HPPL cells infected with pMXs-Neo or with pMXs-Neo-Grhl2 using miRNeasy (Qiagen). Hybridization and data analysis were performed by Miltenyi Biotec using miRXplore. Microarray data are available at GEO under accession number GSE62862.

Acknowledgements

We thank Ms Minako Kuwano and Ms Yumiko Tsukamoto for technical assistance.

Competing interests

The authors declare no competing financial interests.

Author contributions

N.T.: conception and design, financial support, the collection, assembly, analysis and interpretation of data, manuscript writing. S.K.: collection and assembly of data. N.I.: discussion of data. T.M.: financial support, data interpretation, manuscript editing.

Funding

This work is supported by the Ministry of Education, Culture, Sports, Science and Technology, Japan, Grants-in-Aid for Young Scientists (B) for N.T. [22790386] and Grants-in-Aid for Scientific Research (B) for T.M. [21390365, 24390304].

Supplementary material

Supplementary material available online at
http://dev.biologists.org/lookup/suppl/doi:10.1242/dev.113654/-/DC1

References

Antoniou, A., Raynaud, P., Cordi, S., Zong, Y., Tronche, F., Stanger, B. Z., Jacquemin, P., Pierreux, C. E., Clotman, F. and Lemaigre, F. P. (2009). Intrahepatic bile ducts develop according to a new mode of tubulogenesis regulated by the transcription factor SOX9. *Gastroenterology* **136**, 2325-2333.

Barker, N., Bartfeld, S. and Clevers, H. (2010). Tissue-resident adult stem cell populations of rapidly self-renewing organs. *Cell Stem Cell* **7**, 656-670.

Boulter, L., Govaere, O., Bird, T. G., Radulescu, S., Ramachandran, P., Pellicoro, A., Ridgway, R. A., Seo, S. S., Spee, B., Van Rooijen, N. et al. (2012). Macrophage-derived Wnt opposes Notch signaling to specify hepatic progenitor cell fate in chronic liver disease. *Nat. Med.* **18**, 572-579.

Cardinale, V., Wang, Y., Carpino, G., Cui, C.-B., Gatto, M., Rossi, M., Berloco, P. B., Cantafora, A., Wauthier, E., Furth, M. E. et al. (2011). Multipotent stem/progenitor cells in human biliary tree give rise to hepatocytes, cholangiocytes, and pancreatic islets. *Hepatology* **54**, 2159-2172.

Carpentier, R., Suñer, R. E., van Hul, N., Kopp, J. L., Beaudry, J. B., Cordi, S., Antoniou, A., Raynaud, P., Lepreux, S., Jacquemin, P. et al. (2011). Embryonic ductal plate cells give rise to cholangiocytes, periportal hepatocytes, and adult liver progenitor cells. *Gastroenterology* **141**, 1432-1438.e4.

Dorrell, C., Erker, L., Schug, J., Kopp, J. L., Canaday, P. S., Fox, A. J., Smirnova, O., Duncan, A. W., Finegold, M. J., Sander, M. et al. (2011). Prospective isolation of a bipotential clonogenic liver progenitor cell in adult mice. *Genes Dev.* **25**, 1193-1203.

Español-Suñer, R., Carpentier, R., Van Hul, N., Legry, V., Achouri, Y., Cordi, S., Jacquemin, P., Lemaigre, F. and Leclercq, I. A. (2012). Liver progenitor cells yield functional hepatocytes in response to chronic liver injury in mice. *Gastroenterology* **143**, 1564-1575.e7.

Fuchs, E. (2009). Finding one's niche in the skin. *Cell Stem Cell* **4**, 499-502.

Furuyama, K., Kawaguchi, Y., Akiyama, H., Horiguchi, M., Kodama, S., Kuhara, T., Hosokawa, S., Elbahrawy, A., Soeda, T., Koizumi, M. et al. (2011). Continuous cell supply from a Sox9-expressing progenitor zone in adult liver, exocrine pancreas and intestine. *Nat. Genet.* **43**, 34-41.

Hikichi, T., Matoba, R., Ikeda, T., Watanabe, A., Yamamoto, T., Yoshitake, S., Tamura-Nakano, M., Kimura, T., Kamon, M., Shimura, M. et al. (2013). Transcription factors interfering with dedifferentiation induce cell type-specific transcriptional profiles. *Proc. Natl. Acad. Sci. USA* **110**, 6412-6417.

Huang, P., He, Z., Ji, S., Sun, H., Xiang, C., Liu, C., Hu, Y., Wang, X. and Hui, L. (2011). Induction of functional hepatocyte-like cells from mouse fibroblasts by defined factors. *Nature* **475**, 386-389.

Huch, M., Dorrell, C., Boj, S. F., van Es, J. H., Li, V. S. W., van de Wetering, M., Sato, T., Hamer, K., Sasaki, N., Finegold, M. J. et al. (2013). In vitro expansion of single Lgr5+ liver stem cells induced by Wnt-driven regeneration. *Nature* **494**, 247-250.

Kamiya, A., Kakinuma, S., Yamazaki, Y. and Nakauchi, H. (2009). Enrichment and clonal culture of progenitor cells during mouse postnatal liver development in mice. *Gastroenterology* **137**, 1114-1126.e14.

Laudadio, I., Manfroid, I., Achouri, Y., Schmidt, D., Wilson, M. D., Cordi, S., Thorrez, L., Knoops, L., Jacquemin, P., Schuit, F. et al. (2012). A feedback loop between the liver-enriched transcription factor network and miR-122 controls hepatocyte differentiation. *Gastroenterology* **142**, 119-129.

Malato, Y., Naqvi, S., Schürmann, N., Ng, R., Wang, B., Zape, J., Kay, M. A., Grimm, D. and Willenbring, H. (2011). Fate tracing of mature hepatocytes in mouse liver homeostasis and regeneration. *J. Clin. Invest.* **121**, 4850-4860.

Oertel, M., Rosencrantz, R., Chen, Y.-Q., Thota, P. N., Sandhu, J. S., Dabeva, M. D., Pacchia, A. L., Adelson, M. E., Dougherty, J. P. and Shafritz, D. A. (2003). Repopulation of rat liver by fetal hepatoblasts and adult hepatocytes transduced ex vivo with lentiviral vectors. *Hepatology* **37**, 994-1005.

Okabe, M., Tsukahara, Y., Tanaka, M., Suzuki, K., Saito, S., Kamiya, Y., Tsujimura, T., Nakamura, K. and Miyajima, A. (2009). Potential hepatic stem cells reside in EpCAM+ cells of normal and injured mouse liver. *Development* **136**, 1951-1960.

Pan, F. C., Bankaitis, E. D., Boyer, D., Xu, X., Van de Casteele, M., Magnuson, M. A., Heimberg, H. and Wright, C. V. E. (2013). Spatiotemporal patterns of multipotentiality in Ptf1a-expressing cells during pancreas organogenesis and injury-induced facultative restoration. *Development* **140**, 751-764.

Sekiya, S. and Suzuki, A. (2011). Direct conversion of mouse fibroblasts to hepatocyte-like cells by defined factors. *Nature* **156**, 390-393.

Senga, K., Mostov, K. E., Mitaka, T., Miyajima, A. and Tanimizu, N. (2012). Grainyhead-like 2 regulates epithelial morphogenesis by establishing functional tight junctions through the organization of a molecular network among claudin3, claudin4, and Rab25. *Mol. Biol. Cell* **23**, 2845-2855.

Suzuki, A., Zheng, Y.-W., Kaneko, S., Onodera, M., Fukao, K., Nakauchi, H. and Taniguchi, H. (2002). Clonal identification and characterization of self-renewing pluripotent stem cells in the developing liver. *J. Cell Biol.* **156**, 173-184.

Suzuki, A., Sekiya, S., Onishi, M., Oshima, N., Kiyonari, H., Nakauchi, H. and Taniguchi, H. (2008). Flow cytometric isolation and clonal identification of self-renewing bipotent hepatic progenitor cells in adult mouse liver. *Hepatology* **48**, 1964-1978.

Tanimizu, N. and Miyajima, A. (2004). Notch signaling controls hepatoblast differentiation by altering the expression of liver-enriched transcription factors. *J. Cell Sci.* **117**, 3165-3174.

Tanimizu, N., Nishikawa, M., Saito, H., Tsujimura, T. and Miyajima, A. (2003). Isolation of hepatoblasts based on the expression of Dlk/Pref-1. *J. Cell Sci.* **116**, 1775-1786.

Tanimizu, N., Nakamura, Y., Ichinohe, N., Mizuguchi, T., Hirata, K. and Mitaka, T. (2013). Hepatic biliary epithelial cells acquire epithelial integrity but lose plasticity to differentiate into hepatocytes in vitro during development. *J. Cell Sci.* **126**, 5239-5246.

Tarlow, B. D., Finegold, M. J. and Grompe, M. (2014). Clonal tracing of Sox9+ liver progenitors in oval cell injury. *Hepatology* **60**, 278-289.

Xu, H., He, J.-H., Xiao, Z.-D., Zhang, Q.-Q., Chen, Y.-Q., Zhou, H. and Qu, L.-H. (2010). Liver-enriched transcription factors regulate microRNA-122 that targets CUTL1 during liver development. *Hepatology* **52**, 1431-1442.

Zhou, Q., Law, A. C., Rajagopal, J., Anderson, W. J., Gray, P. A. and Melton, D. A. (2007). A multipotent progenitor domain guides pancreatic organogenesis. *Dev. Cell* **13**, 103-114.

Zong, Y., Panikkar, A., Xu, J., Antoniou, A., Raynaud, P., Lemaigre, F. and Stanger, B. Z. (2009). Notch signaling controls liver development by regulating biliary differentiation. *Development* **136**, 1727-1739.

Fig. S1

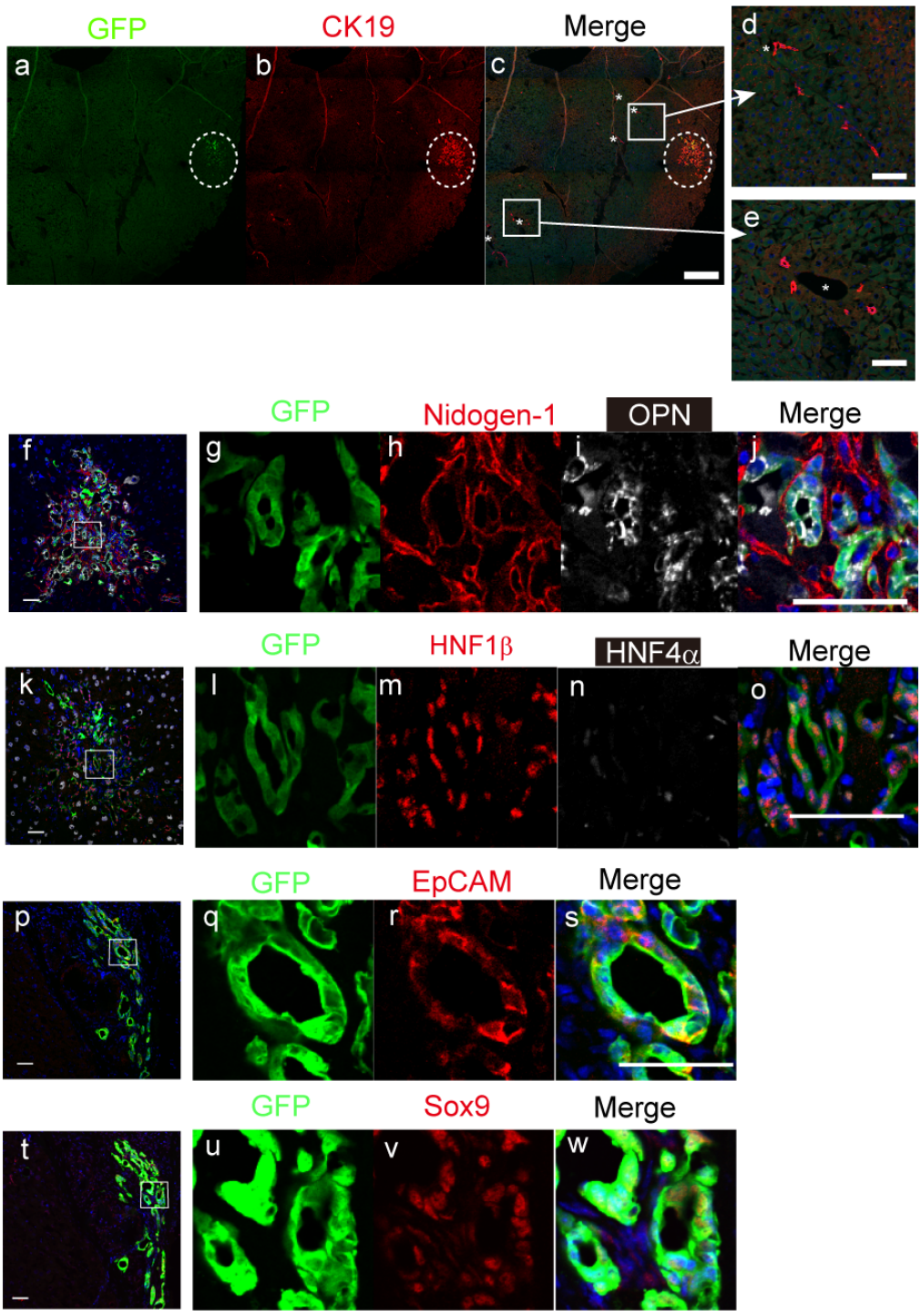

Fig. S1. Adult clone 1 differentiates to cholangiocyte-like cells and forms ductular structures in the recipient liver. GFP$^+$ donor cells form ductular structures, surrounded by dotted circles, apart from portal veins (asterisks). Boxes in panel c are enlarged in panels d and e. Bars in panel c and d&e represent 500 and 100 μm, respectively. GFP$^+$ donor cells express cholangiocyte markers including OPN, HNF1β, EpCAM and Sox9 but not a hepatocyte marker HNF4α. GFP$^+$ ductular structures are associated with the ECM layer recognized with Nidogen-1. Bars in panels a, f, p, and t represent 100 μm. Bars in panels e, j, o, and s represent 50 μm.

Fig. S2

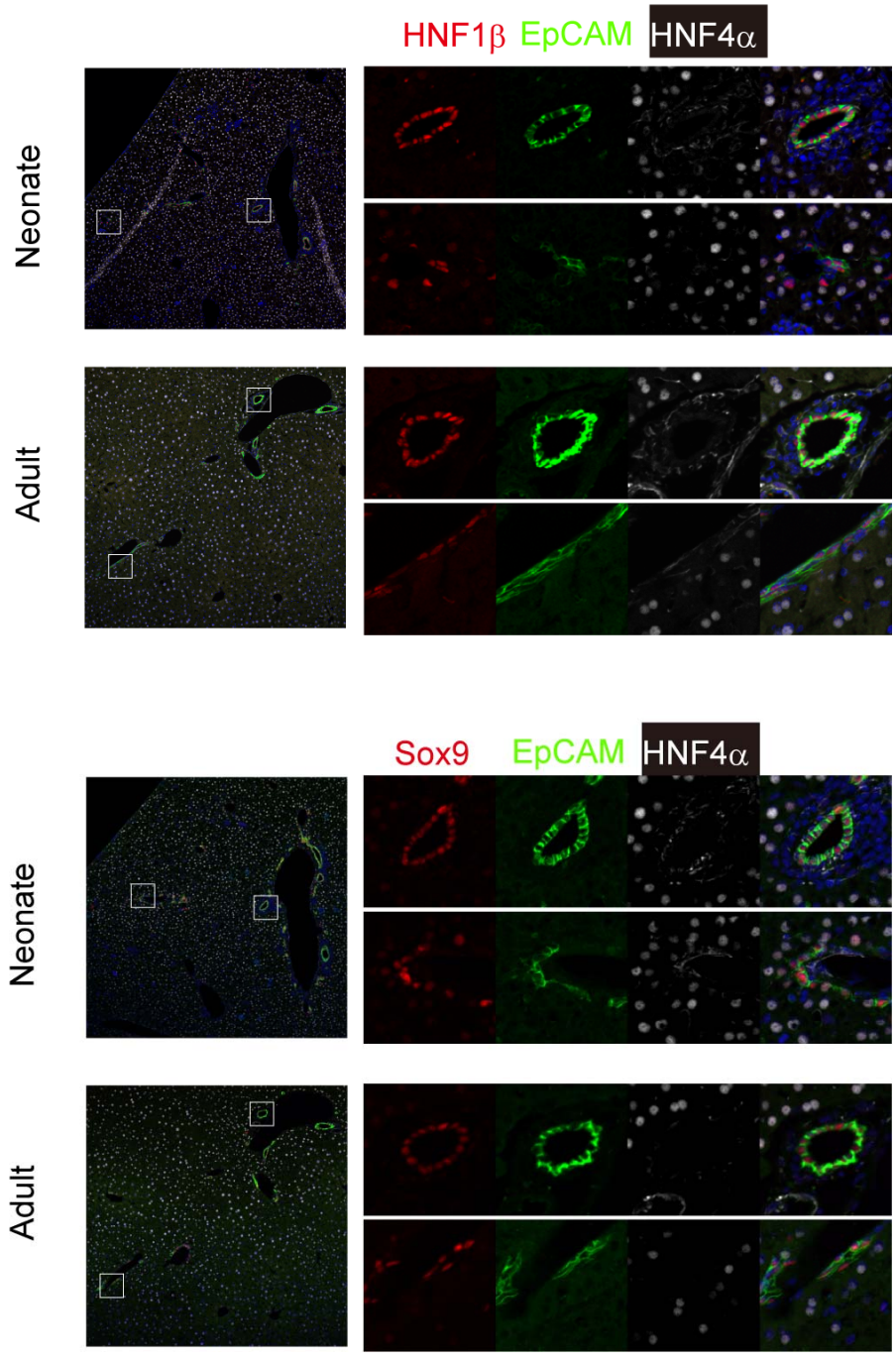

Fig. S2. Neonatal and adult EpCAM^{+} cells are positive for HNF1β and Sox9.

Fig. S3

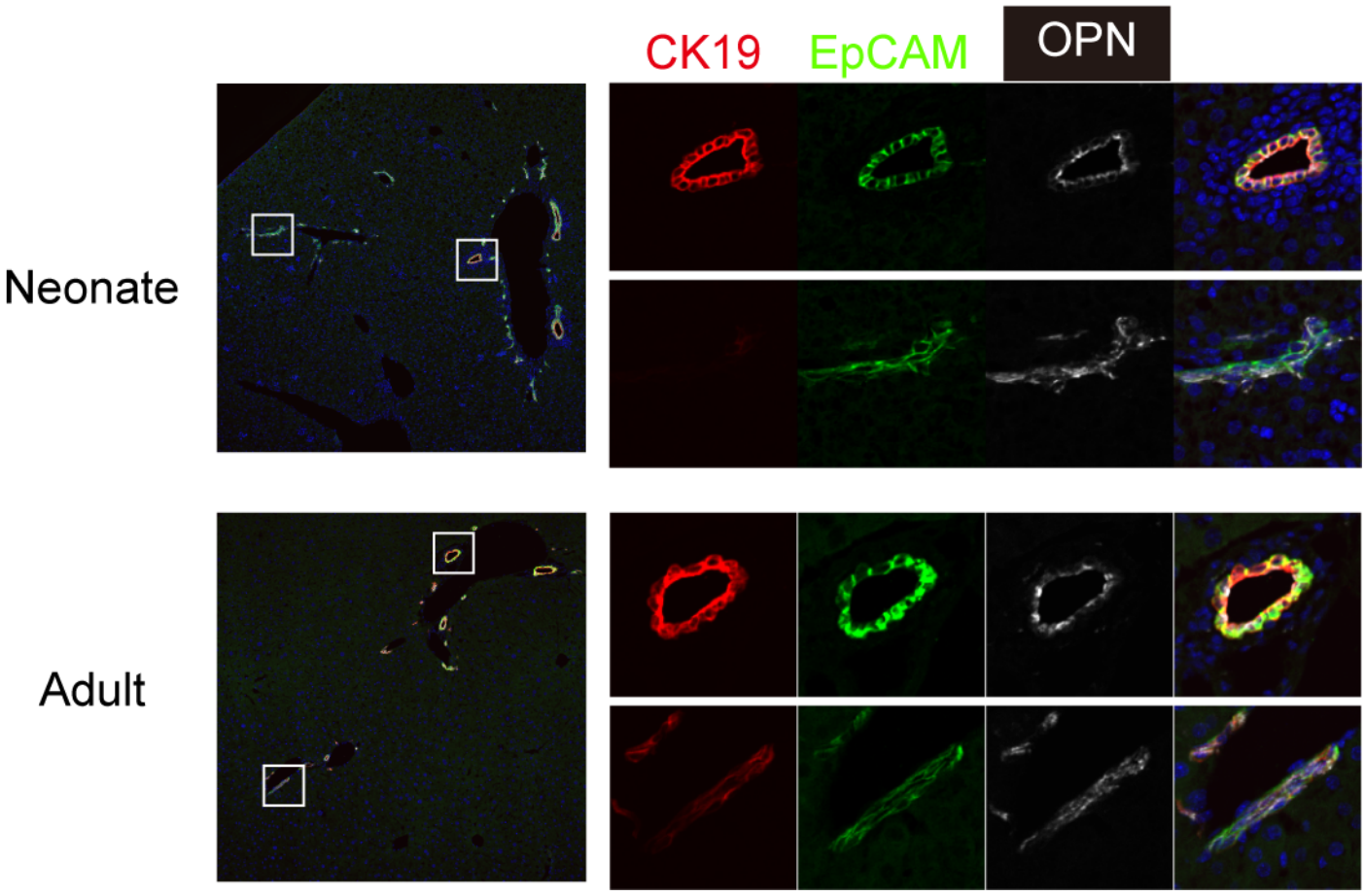

Fig. S3. Neonatal small ductules in the periphery are negative for CK19.

Fig. S4

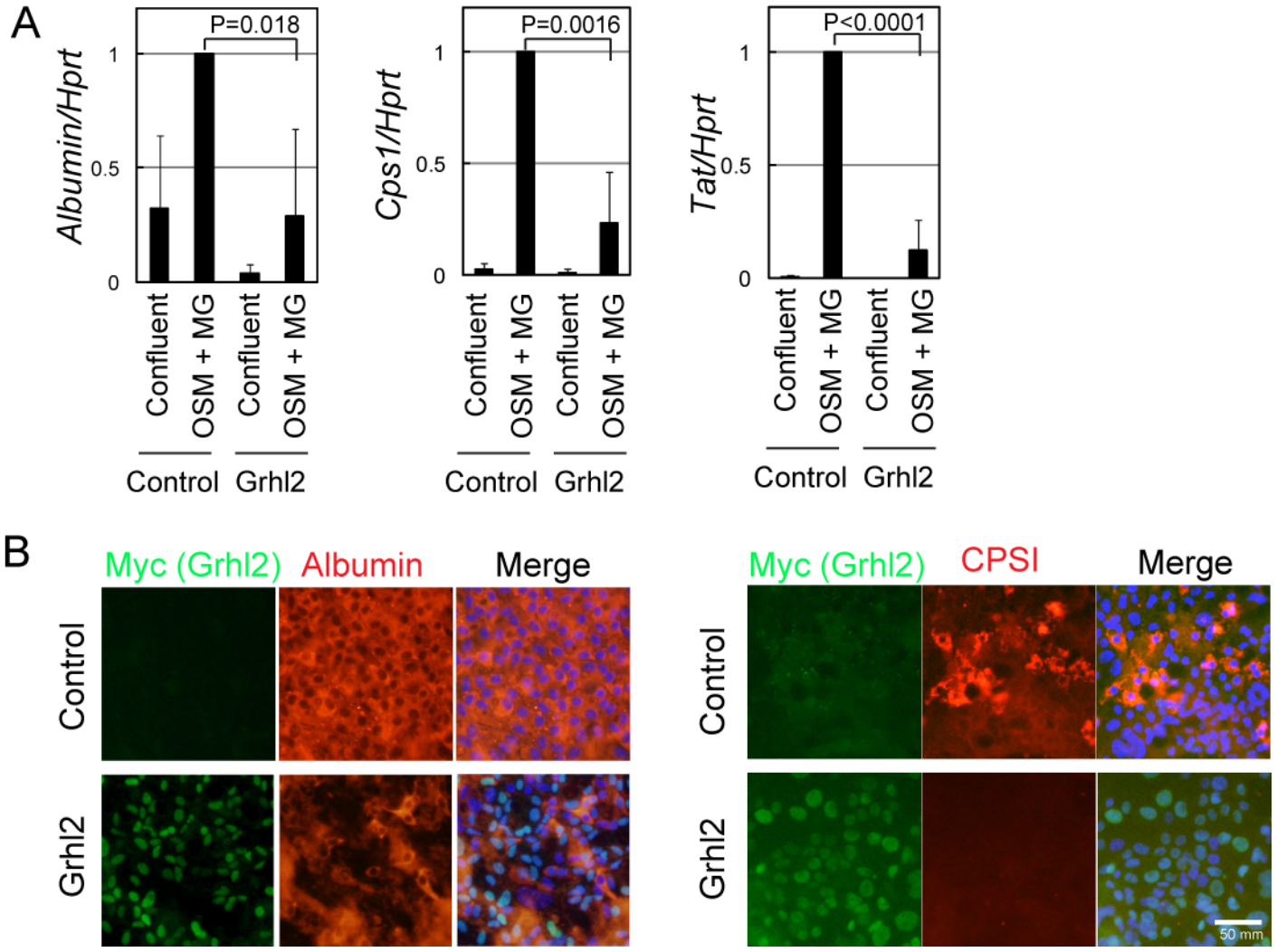

Fig. S4. Grhl2 inhibits hepatocytic differentiation of liver progenitors. HPPL, bipotential liver progenitor cell line, was introduced with Grhl2 by using a retrovirus vector. Hepatocytic differentiation was induced by oncostatin M (OSM) and Matrigel (MG). Grhl2 inhibits induction of *Albumin*, *Cps1*, and *Tat* (A) as well as ALBUMIN and CPSI (B). A bar represents 50 μm.

Fig. S5.

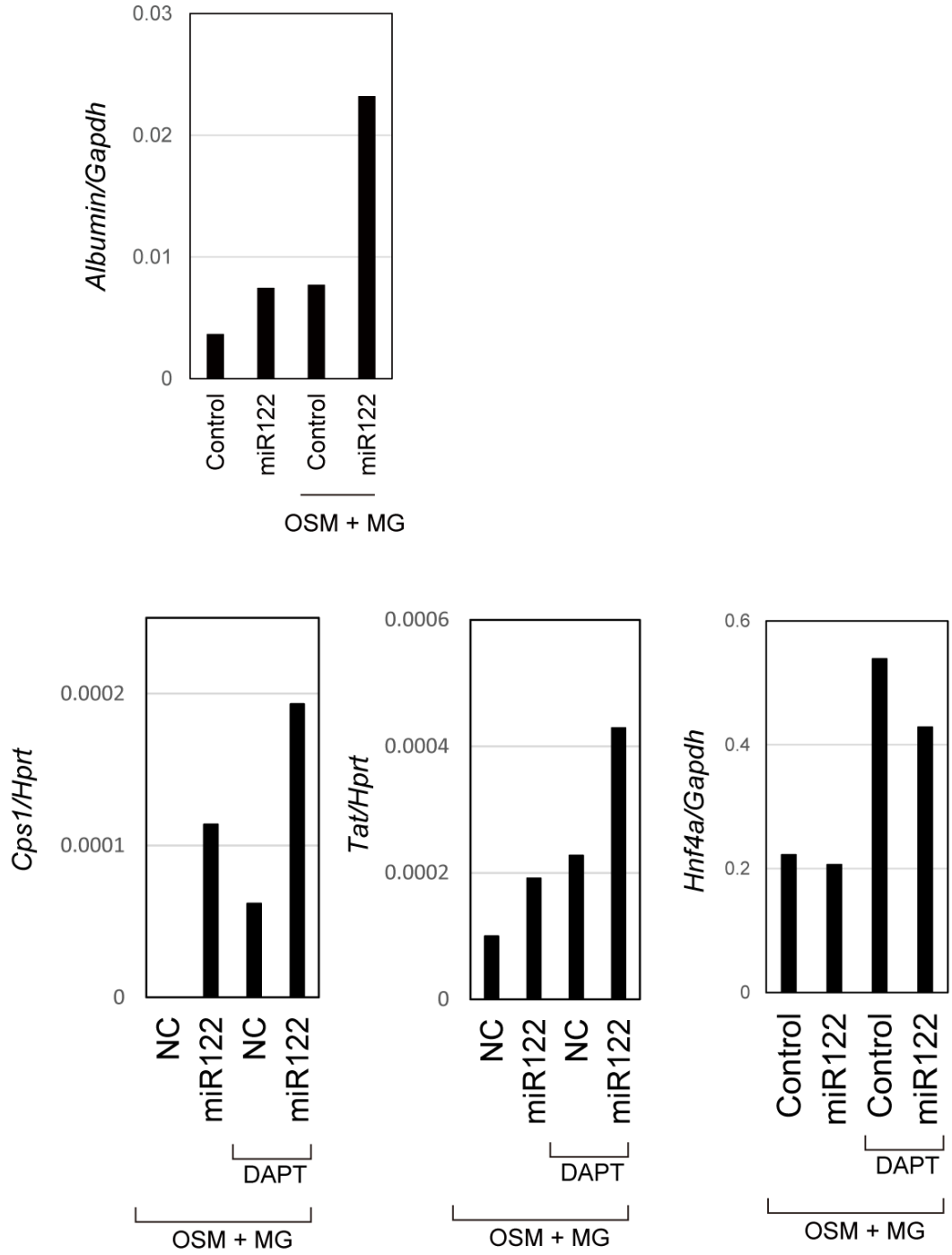

Fig. S5. miR122 promotes hepatocytic differentiation of adult EpCAM$^+$ cells. miR122 slightly upregulates hepatocyte markers. EpCAM$^+$ cells isolated from adult livers were cultured on gelatin coated dishes. They were transfected with miR122 and then treated with OSM and MG. For inducing *Cps1* and *Tat*, EpCAM$^+$ cells were also treated with DAPT, a γ-secretase inhibitor, and potential inhibitor of the Notch signaling pathway.

Fig. S6

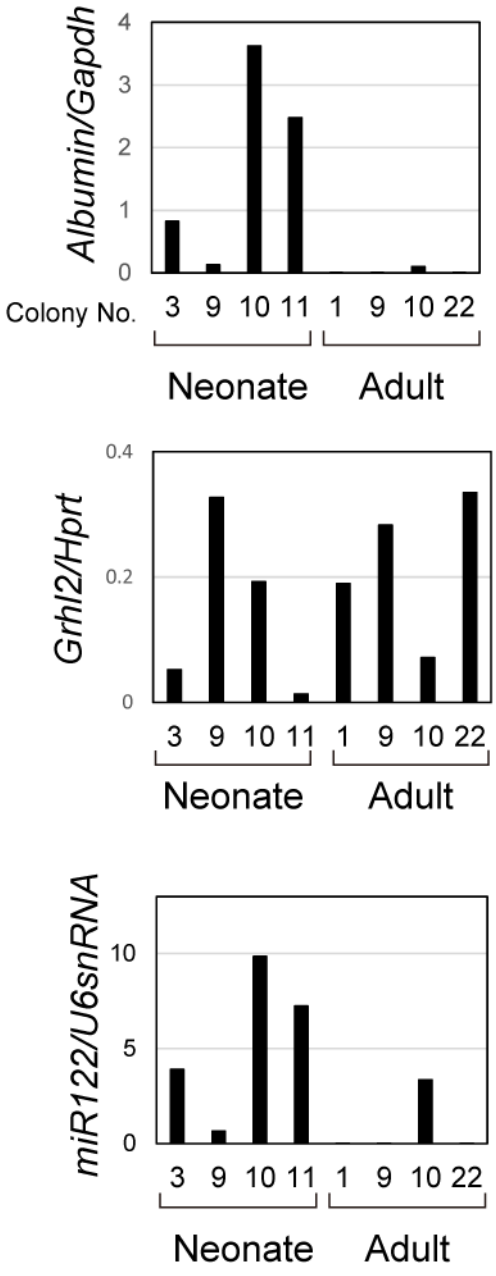

Fig. S6. Expression of Albumin, Grhl2, and miR122 in colonies derived from neonatal and adult EpCAM$^+$ cells.

Table S1. Primary Antibodies

Antibody	Company	Cat. Number	Host animal	Method	Dilution
ALB	Bethyl laboratory	A90-234A	goat	IF	1:1000
CD16/32	BD Pharmingen	553141	rat	FACS	1:1000
CD31	Biolegend	102501	rat	IF	1:1000
CD31 (APC-conjugated)	BD Pharmingen	551262	rat	FACS	1:1000
CD45 (APC-conjugated)	BD Pharmingen	559864	rat	FACS	1:1000
C/EBPα	SantaCruz Biotechnology Inc.	sc-61	rabbit	IF	1:200
CPSI	Santa Cruz Biotechnology Inc.	sc-10516	goat	IF	1:200
Cytokeratin 19	Tanimizu et al. 2003		rabbit	IF	1:2000
EpCAM	BD Pharmingen	552370	rat	IF	1:500
EpCAM (FITC or APC-conjugated)	Biolegend	118208 118213	rat	FACS	1:1000
GFP	MBL	598	rabbit	IF	1:1000
GFP	Nakarai Tesk	GF090R	rat	IF	1:1000
GRHL2	Sigma-Aldrich	HPA004820	rabbit	IF	1:1000
HNF1β	SantaCruz Biotechnology Inc.	sc-22840	rabbit	IF	1:200
HNF4α	SantaCruz Biotechnology Inc.	sc-8987	rabbit	IF	1:200
HNF4α	SantaCruz Biotechnology Inc.	sc-6557	goat	IF	1:200
Myc-tag	Millipore	05-074	mouse	IF	1:1000
Nidogen-1	Millipore	MAB1946	rat	IF	1:1000
Osteopontin	R&D systems	AF808	goat	IF	1:600
SOX9	Millipore	AB5535	rabbit	IF	1:3000
TER119 (APC/Cy7-conjugated)	Biolegend	116223	rat	FACS	1:1000

Table S2. Primers used for PCR

Gene name		Sequence
Albumin	Sense	5′-GAA AGC CCA CTG TCT TAG TG-3′
	Antisense	5′-GGG TGT AGC GAA CTA GAA TG-3′
Cyp1a2	Sense	5′-CCCTGCCCTTCAGTGGTACA-3′
	Antisense	5′-AAGCTGTAGAGGTCTGGTCG-3′
Cyp2b10	Sense	5′-GTTGAGCCAACCTTCAAGGAA-3′
	Antisense	5′-AAGAGCTCAAACATCTGGCTG-3′
Cyp2d10	Sense	5′-GATCCCAAGGTGTGGTCCTT-3′
	Antisense	5′-GCAGGAGTATGGGGAACATA-3′
CPSI	Sense	5′-ACT GAG AGA TGC TGA CCC TA-3′
	Antisense	5′-CCT GGA AAT TGG TGA GGA GA-3′
GAPDH	Sense	5′-ACC ACA GTC CAT GCC ATC AC-3′
	Antisense	5′-TCC ACC ACC CTG TTG CTG TA-3′
G6pc	Sense	5’-CCA ACG TAT GGA TTC CGG TG-3’
	Antisense	5’-TCC CAG GTT TTT GAA GAG GC-3’
GFP	Sense	5′-CTGAAGTTCATCTGCACCAC-3′
	Antisense	5′-TTGAAGTTCACCTTGATGCC-3′
Pepck	Sense	TTGATGCCCAAGGCAACTTA
	Antisense	ACGGCCACCAAAGATGATAC
TAT	Sense	5′-GAG GAG TGT GAC AAA TAG GC-3′
	Antisense	5′-AGA GGA CAC TCC TGT GTC AG-3′
Tdo2	Sense	5′-TGAGTAAAGGTGAACGACGAC-3′
	Antisense	5′-AGCCGACTGAGAATCCTGTA-3′

Table S3.

Click here to Download Table S3